Analysis of Discontinuities in an Open Dielectric Slab Waveguide by Combination of Finite and Boundary Elements

KOICHI HIRAYAMA AND MASANORI KOSHIBA, SENIOR MEMBER, IEEE

Abstract—**A combination of the finite element and boundary element methods is proposed for the solution of arbitrarily shaped discontinuities in an open dielectric slab waveguide. The discontinuity region is divided into two regions. One is a finite region with arbitrary inhomogeneities, and the other is a semi-infinite and homogeneous region. The finite element and boundary element methods are applied to the former and the latter region, respectively. For uniform waveguide regions connected to discontinuities, analytical solutions in which both the guided and the radiated modes are taken into account are used. To show the validity and usefulness of this approach, computed results are given for several kinds of discontinuities, and the accuracy of the solutions is investigated in detail.**

I. Introduction

DISCONTINUITIES in an open dielectric slab waveguide play an important role in designing optical- and millimeter-wave components. Various theoretical methods for the solution of dielectric slab waveguide discontinuities have been developed [1]–[23]. Although these methods are very useful for a step discontinuity or a cascade of steps, it seems to be difficult to apply them to arbitrarily shaped discontinuities. Recently, the integral equation method (IEM) [24]–[27], the boundary element method (BEM) [28], and the finite element method (FEM) [29]–[32] have been presented for the solution of arbitrarily shaped discontinuities. In [24]–[27] using the IEM, however, only the weakly guiding structure is considered. Also, the BEM cannot be effectively applied to a problem involving inhomogeneous media. The FEM is very useful for the arbitrarily shaped discontinuities including inhomogeneous media. However, in [29], although uniform waveguide regions connected to discontinuities are treated analytically as unbounded configurations, discontinuity regions to which the FEM is applied are treated as corresponding bounded ones. In [30]–[32], both uniform waveguide regions and discontinuity regions are treated as bounded configurations.

In this paper, we present a novel numerical approach based on a combination of finite and boundary elements for the solution of discontinuities in an open dielectric slab waveguide. The discontinuity region is divided into two regions. One is a finite region with arbitrary inhomogeneities; the other is a semi-infinite and homogeneous region. The FEM and the BEM are applied to the former and the latter region, respectively. The finite element can be combined with the boundary element on the common nodal points because these two methods are discretized in the same way. Also, analytical solutions in which both the guided and the radiated modes are taken into account are used for uniform waveguide regions connected to discontinuities. To show the validity and usefulness of this formulation, computed results are given for a step, a gap, and a triangular rib. The accuracy of the solution is investigated in detail.

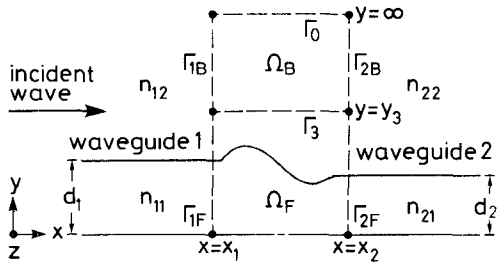

Fig. 1 Geometry of problem.

II. Basic Equations

Consider a symmetric mode excitation of the symmetric slab waveguide shown in Fig. 1, where the boundary Γ_0 is placed at infinity ($y=\infty$) and the boundary $\Gamma_i=\Gamma_{iF}+\Gamma_{iB}$ connects the discontinuities to the uniform waveguide i ($i=1,2$). The region Ω_F surrounded by the boundary $\Gamma_F=\Gamma_{1F}+\Gamma_{2F}+\Gamma_3$ and the symmetry plane ($y=0$) completely encloses the discontinuities. The region Ω_B is surrounded by the boundaries $\Gamma_B=\Gamma_{1B}+\Gamma_{2B}+\Gamma_3$ and Γ_0, and d_i and n_{ij} ($j=1,2$) are the half thickness and the refractive index of waveguide i ($n_{i1}>n_{i2}$), respectively.

Assuming that there is no variation in the z direction, we obtain the following basic equation:

$$\frac{1}{p}\left(\frac{\partial^2\phi}{\partial x^2}+\frac{\partial^2\phi}{\partial y^2}\right)+k_0^2q\phi=0 \tag{1}$$

Manuscript received June 13, 1988; revised November 7, 1988
The authors are with the Department of Electronic Engineering, Hokkaido University, Sapporo, 060 Japan.
IEEE Log Number 8826056.

0018-9480/89/0400-0761$01.00 ©1989 IEEE

where

$$\phi = E_z \qquad p = 1 \qquad q = n^2 \qquad \text{for TE modes} \tag{2a}$$

$$\phi = H_z \qquad p = n^2 \qquad q = 1 \qquad \text{for TM modes} \tag{2b}$$

$$k_0 = 2\pi/\lambda. \tag{3}$$

Here E_z and H_z are the z components of the electric and magnetic fields, respectively, and λ is the wavelength of a plane wave in free space.

We define ψ on Γ_1, Γ_2, and Γ_3 as follows:

$$\psi = -\lambda \partial\phi/\partial x \qquad \text{on } \Gamma_1 \tag{4a}$$

$$\psi = \lambda \partial\phi/\partial x \qquad \text{on } \Gamma_2 \tag{4b}$$

$$\psi = -\lambda \partial\phi/\partial y \qquad \text{on } \Gamma_3. \tag{4c}$$

III. Mathematical Formulation

A. Finite Element Approach for Ω_F

Dividing the region Ω_F into a number of quadratic triangular elements [29]–[33], using a Galerkin procedure on (1), considering the contributions of all elements, and eliminating internal variables, namely the nodal points in Ω_F except Γ_F [31], [33], we obtain the following small-sized matrix equation:

$$[A]\{\phi\}_F = [B]\{\psi\}_F \tag{5}$$

where the components of the $\{\phi\}_F$ and $\{\psi\}_F$ vectors are the values of ϕ and ψ at the nodal points on Γ_F, respectively, and $[A]$ and $[B]$ are the finite element matrices [29]–[33].

B. Boundary Element Approach for Ω_B

Applying the BEM with quadratic line element [34] to the region Ω_B and considering the radiation condition on Γ_0, we obtain the following matrix equation:

$$[H]\{\phi\}_B = [G]\{\psi\}_B \tag{6}$$

where the components of the $\{\phi\}_B$ and $\{\psi\}_B$ vectors are the values of ϕ and ψ at the nodal points on Γ_B, respectively, and $[H]$ and $[G]$ are the boundary element matrices [34].

C. Analytical Approach

Assuming that the fundamental mode ($m = 0$) of unit amplitude is incident from the left side of waveguide 1 in Fig. 1, ϕ on Γ_i ($i = 1,2$) may be expressed analytically as

$$\phi_i = \delta_{i1} 2\exp(-j\beta_{10}x_1) f_{10}(y) + \sum_{m=0}^{M_i-1} \frac{f_{im}(y)}{-j\beta_{im}\lambda} \int_0^\infty g_{im}(y')\psi_i(x_i, y')\, dy' + \int_0^\infty \frac{f_i(\rho, y)}{-j\beta_i(\rho)\lambda} \int_0^\infty g_i(\rho, y')\psi_i(x_i, y')\, dy'\, d\rho, \qquad i = 1,2 \tag{7}$$

where ϕ_i and ψ_i are the values of ϕ and ψ on Γ_i, respectively, δ_{i1} is the Kronecker δ, and M_i is the number of guided modes in waveguide i. A summary of the mode functions $f_{im}(y)$, $g_{im}(y)$, $f_i(\rho, y)$, and $g_i(\rho, y)$ and of the propagation constants β_{im} and $\beta_i(\rho)$ is given in the Appendix.

We discretize (7) as follows:

$$\{\phi\}_i = \delta_{i1}\{f\}_1 + [Z]_i\{\psi\}_i \tag{8}$$

where

$$\{f\}_1 = 2\exp(-j\beta_{10}x_1)\{f_0\}_1 \tag{9a}$$

$$[Z]_i = \sum_{m=0}^{M_i-1} \{f_m\}_i \frac{1}{-j\beta_{im}\lambda} \{\hat{g}_m\}_i^T + \int_0^\infty \{f(\rho)\}_i \frac{1}{-j\beta_i(\rho)\lambda} \{\hat{g}(\rho)\}_i^T d\rho \tag{9b}$$

$$\{\hat{g}_m\}_i = \sum_{e'} \int_{e'} g_{im}(y')\{N\}_i\, dy' \tag{9c}$$

$$\{\hat{g}(\rho)\}_i = \sum_{e'} \int_{e'} g_i(\rho, y')\{N\}_i\, dy'. \tag{9d}$$

Here the components of the $\{f_m\}_i$ and $\{f(\rho)\}_i$ vectors are the values of $f_{im}(y)$ and $f_i(\rho, y)$ at the nodal points on Γ_i, respectively, $\{N\}_i$ is the shape function vector [29]–[34] on Γ_i, and the superscript T denotes a transpose.

D. Combination of Finite and Boundary Elements

From (5), (6), and (8), we obtain the following final matrix equation:

$$\left[\begin{array}{c|c} [A'] & -[B'] \\ [H'] & -[G'] \\ \hline [1][0][0] & -[Z]_1\ [0]\ [0] \\ [0][1][0] & [0]\ -[Z]_2[0] \end{array}\right] \left[\begin{array}{c} \{\phi\}_1 \\ \{\phi\}_2 \\ \{\phi\}_3 \\ \hline \{\psi\}_1 \\ \{\psi\}_2 \\ \{\psi\}_3 \end{array}\right] = \left[\begin{array}{c} \{0\} \\ \{0\} \\ \hline \{f\}_1 \\ \{0\} \end{array}\right] \tag{10}$$

where the components of the $\{\phi\}_i$ and $\{\psi\}_i$ vectors are the values of ϕ and ψ at the nodal points on Γ_i ($i = 1,2,3$), respectively, [1] is a unit matrix, [0] is a null matrix, and $\{0\}$ is a null vector. The columns of $[A']$ and $[B']$ corresponding to the nodal points on Γ_F are the same as those of $[A]$ and $[B]$, respectively, and the others are zero. Similarly, the columns of $[H']$ and $[G']$ corresponding to the nodal points on Γ_B are the same as those of $[H]$ and $[G]$, respectively, and the others are zero.

The solutions of (10) allow the determination of the normalized reflected power $|R_m|^2$ and the normalized transmitted power $|T_m|^2$ of the mth mode, and the normal-

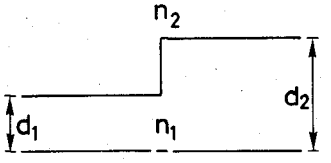

Fig. 2. Step discontinuity.

ized radiated power P_{ir} in waveguide i as follows:

$$|R_m|^2 = \frac{\beta_{1m}}{\beta_{10}} \left| \delta_{m0} \exp(-j\beta_{10}x_1) + \frac{1}{-j\beta_{1m}\lambda} \{\hat{g}_m\}_1^T \{\psi\}_1 \right|^2 \tag{11a}$$

$$|T_m|^2 = \frac{\beta_{2m}}{\beta_{10}} \left| \frac{1}{-j\beta_{2m}\lambda} \{\hat{g}_m\}_2^T \{\psi\}_2 \right|^2 \tag{11b}$$

$$P_{ir} = \frac{1}{\beta_{10}\lambda} \{\psi\}_i^\dagger \int_0^{n_{i2}k_0} \frac{1}{\beta_i(\rho)\lambda} \{\hat{g}(\rho)\}_i \cdot \{\hat{g}(\rho)\}_i^T d\rho \{\psi\}_i, \qquad i=1,2 \tag{11c}$$

where the dagger denotes a Hermitian conjugate, and the integral with respect to ρ in (11c) is calculated numerically.

IV. Computed Results

For numerical computation, introducing a parameter D, we divide the integrals with respect to y in the boundary element approach into two parts, that is, those in $y_3 \leqslant y \leqslant D$ (the boundary Γ_3 on which the finite element and the boundary element are combined is located at $y = y_3$) and those in $D \leqslant y < \infty$. Also, we divide the integrals with respect to y in the analytical approach into two parts, that is, those in $0 \leqslant y \leqslant D$ and those in $D \leqslant y < \infty$. In each approach, the first part of the integrals is calculated analytically and the second part can be neglected by choosing the value of D adequately. Furthermore, introducing a parameter c_i, we divide the integrals with respect to ρ in the analytical approach into three parts, that is, those in $0 \leqslant \rho \leqslant n_{i2}k_0$ (propagating part), those in $n_{i2}k_0 \leqslant \rho \leqslant c_i n_{i2}k_0$ (nonpropagating part), and those in $c_i n_{i2}k_0 \leqslant \rho < \infty$ (nonpropagating part), where the first two parts are calculated numerically and the last part can be neglected by choosing the value of $c_i (c_i > 1)$ adequately. For simplicity the relation $c_1 = c_2 \equiv c$ is used below. Also, a double-exponential formula [35] is used for the numerical integration over ρ.

First, to check the validity of our approach, we consider a step discontinuity as shown in Fig. 2, where $n_1 = \sqrt{5}$, $n_2 = 1$, $d_2 = \lambda/2\pi$, and the fundamental TE mode incidence is assumed. Convergence of the solution is checked by changing the four parameters, namely, element division and values of c, D, and y_3. Three element divisions used in this calculation are shown in Fig. 3.

Table I shows the variation of solutions with element division, where $c = 4$, $D = 3\lambda$, $y_3 = 2\lambda$, and P_r represents total radiated power, namely $P_r = P_{1r} + P_{2r}$. The difference between the solutions for the divisions in Fig. 3(a) and (b) is very small.

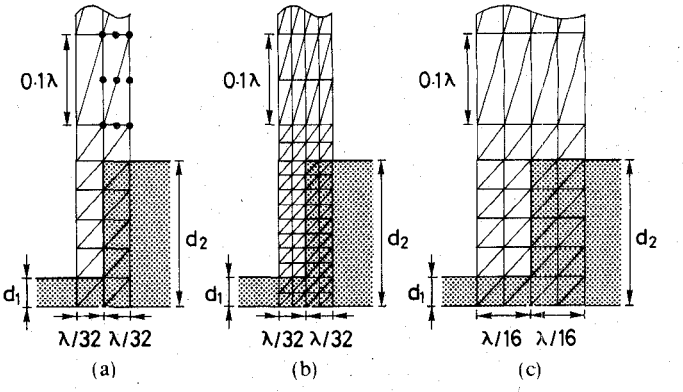

Fig. 3. Element divisions of a step ($d_1/d_2 = 0.2$).

TABLE I
Comparison Between Solutions for the Divisions in Fig. 3(a) and (b)

d_1/d_2	division	$\lvert R_0\rvert^2$	π - ArgR$_0$	$\lvert T_0\rvert^2$	-ArgT$_0$	P_r
0.04	Fig. 3 (a)	0.0100	0.3073	0.3620	0.0581	0.6278
	Fig. 3 (b)	0.0100	0.3075	0.3620	0.0582	0.6278
0.2	Fig. 3 (a)	0.0416	0.0884	0.8865	0.0066	0.0715
	Fig. 3 (b)	0.0416	0.0886	0.8866	0.0066	0.0715

Fig. 4 shows the reflected power, the radiated power, and the phase of reflection coefficient versus $1/c$, where $D = 3\lambda$ and $y_3 = 2\lambda$. The solid and broken lines are for the divisions in Fig. 3(a) and (c), respectively. The variation of the reflected and radiated powers with the value of c is very small. All the solutions converge as $1/c$ approaches zero. The solutions for the division in Fig. 3(c) converge faster than those for the division in Fig. 3(a). In the case where $d_1/d_2 = 0.2$ (Fig. 4(b)), the convergent values for the divisions in Fig. 3(a) and (c) agree well in the reflected power and the phase of reflection coefficient, but differ slightly in the radiated power. This is because the power conservation error increases with the distance between a step and a boundary Γ_i $(i = 1,2)$. For $c = 8$, for example, the power conservation errors for the divisions in Fig. 3(a) and (c) are about 0.039 percent and 0.059 percent, respectively. The difference between these errors is almost equal to the difference between the radiated powers calculated by using the divisions in Fig. 3(a) and (c). In the case where $d_1/d_2 = 0.04$ (Fig. 4(a)), on the other hand, all the convergent values for the divisions in Fig. 3(a) and (c) differ. This is because the field of the guided mode in waveguide 1 extends widely over the y direction. In this case 3λ is not adequate for the value of D. The magnitude of the guided mode at $y = 3\lambda$ normalized by that at $y = 0$ in waveguide 1 is about 0.05 for $d_1/d_2 = 0.04$, whereas it is about 10^{-6} for $d_1/d_2 = 0.2$.

Figs. 5 and 6 show the normalized powers and the phases of the reflection and transmission coefficients versus λ/D, respectively, where $c = 4$, $y_3 = D - \lambda$, and the division in Fig. 3(c) is used. The solid lines represent

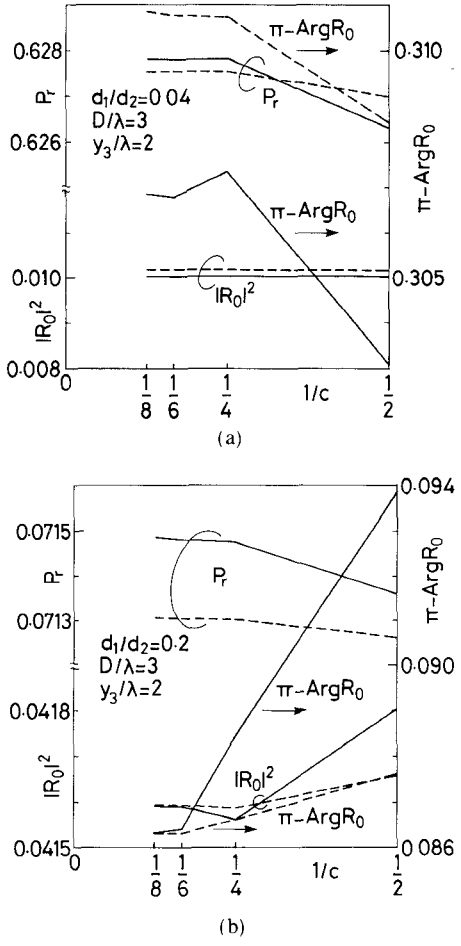

Fig. 4. Normalized power and phase of reflection coefficient versus $1/c$ for a step. The solid and broken lines show the solutions for the divisions in Fig. 3(a) and (c), respectively.

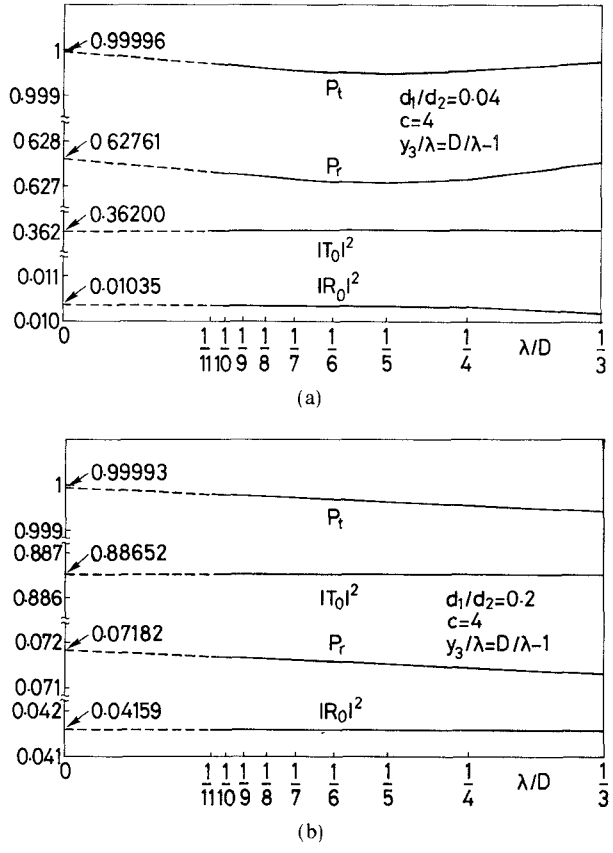

Fig. 5. Normalized power versus λ/D for a step.

computed results and the broken lines are the regression lines calculated from the results of $D/\lambda = 7$, 8, 9, 10, and 11. The extrapolated values at $D \to \infty$ are also shown in Figs. 5 and 6. The variation of solutions with the value of D is very small except for the phase of the reflection coefficient for $d_1/d_2 = 0.04$. In the case where $d_1/d_2 = 0.2$, as shown in Figs. 5(b) and 6(b), the power conservation error decreases with the value of D and the radiated power increases by almost the same amount, but the other solutions remain almost unchanged over $3 \leqslant D/\lambda \leqslant 11$. This fact also holds in the range of $D/\lambda \geqslant 5$ for $d_1/d_2 = 0.04$, as shown in Figs. 5(a) and 6(a), while in the range of $D/\lambda \leqslant 5$ it does not hold due to the wide extension of the guided mode in waveguide 1. Consequently, it seems that several times the free-space wavelength for the value of D yields accurate solutions, and that the extrapolated values at $D \to \infty$ yield more accurate ones. For the finite value of D, poor estimation of radiated power is caused by neglecting the contributions from the electromagnetic fields in the region $y > D$ on Γ_1 and Γ_2.

Table II shows the variation of solutions with the position of Γ_3 ($y = y_3$). The solutions hardly depend on the value of y_3.

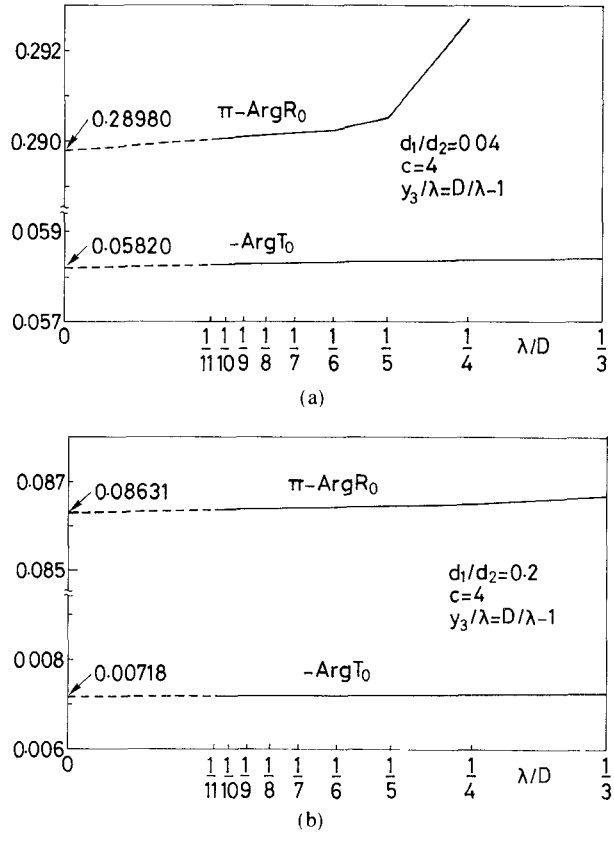

Fig. 6. Phases of reflection and transmission coefficients versus λ/D for a step.

TABLE II
VARIATION OF SOLUTIONS WITH POSITION OF THE BOUNDARY Γ_3 COMBINING FINITE AND BOUNDARY ELEMENTS

d_1/d_2	y_3/λ	$\lvert R_0\rvert^2$	π - ArgR_0	$\lvert T_0\rvert^2$	-ArgT_0	P_r
0.04	1	0.0103	0.2901	0.3620	0.0582	0.6271
	2	0 0103	0.2902	0.3620	0.0583	0.6271
	3	0.0103	0.2903	0.3620	0 0583	0 6271
	4	0.0103	0.2905	0.3620	0.0584	0.6271
0.2	1	0.0416	0.0863	0.8865	0.0072	0.0715
	2	0.0416	0.0864	0.8865	0.0072	0.0715
	3	0.0416	0.0864	0.8865	0.0072	0.0715
	4	0.0416	0.0865	0.8865	0.0072	0.0715

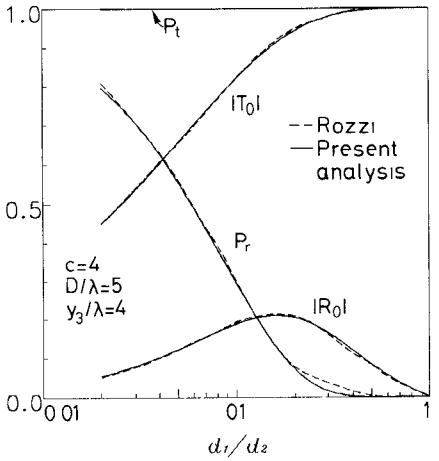

(a)

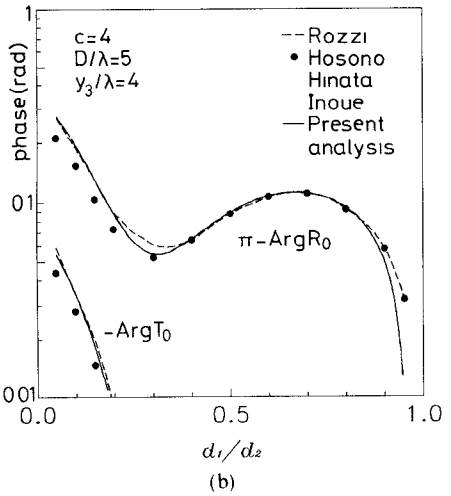

(b)

Fig. 7. Scattering characteristics of a step.

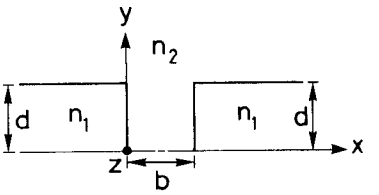

Fig. 8. Gap discontinuity.

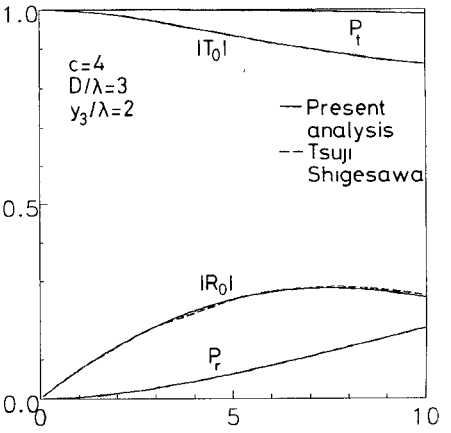

(a)

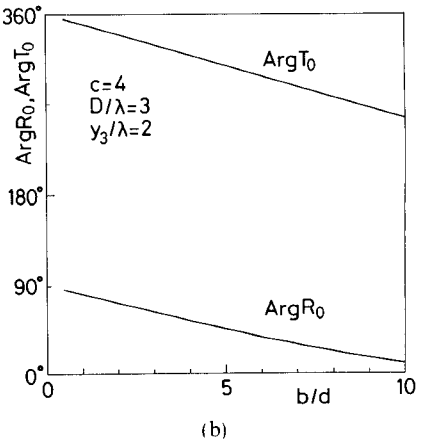

(b)

Fig. 9. Scattering characteristics of a gap.

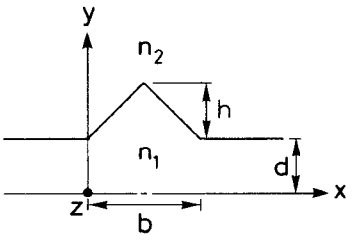

Fig. 10. Triangular rib.

Fig. 7 shows the scattering characteristics of a step. Our results agree well with those of Rozzi [6] and Hosono *et al.* [12].

Next, we consider a gap as shown in Fig. 8, where $n_1 = 2.236$, $n_2 = 1$, $d = \lambda/2\pi$, and the fundamental TE mode incidence is assumed. The scattering characteristics are shown in Fig. 9.

Finally, we consider a triangular rib as shown in Fig. 10, where $n_1 = 3.4$, $n_2 = 1$, $d = 0.075\lambda$, $h/d = 1$ or 0.5, and the fundamental TM mode incidence is assumed. The scattering characteristics are shown in Fig. 11.

For both cases, the guided modes are well confined inside and near the core, and therefore 3λ is sufficient for

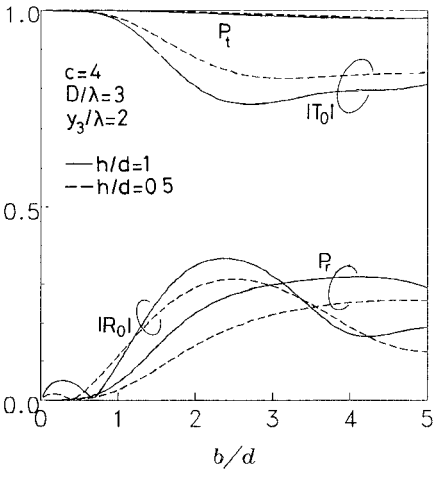

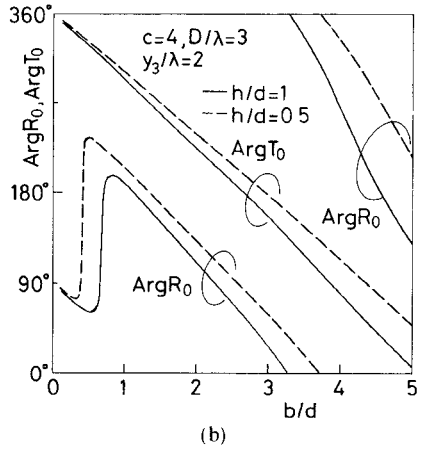

Fig. 11. Scattering characteristics of a triangular rib.

the value of D. The reference planes for the phase of the reflection and transmission coefficients are $x=0$ and $x=b$ (See Figs. 8 and 10), respectively, and the distance between the discontinuity and the boundary Γ_i $(i=1,2)$ is $\lambda/32$.

It is found from Fig. 9 that the phases decrease linearly as the gap becomes wide, and that our results for the magnitude of the reflection coefficient agree well with those of Tsuji and Shigesawa [21], [22].

Note in Fig. 11 that the phase of the reflection coefficient rapidly becomes large and the magnitude becomes a minimum near $b/d=0.7$ or 0.4 in $h/d=1$ or 0.5, respectively, and that a significant amount of radiation, more than 20 percent, appears for $b/d \gtrsim 2$ or 3 in $h/d=1$ or 0.5, respectively. Also, a power conservation error of about 2 percent exists near $b/d=5$ in both cases of $h/d=1$ and 0.5. This is due to the fact that the estimated value for the total radiated power is about 2 percent smaller, while the reflection and transmission coefficients are both obtained with sufficient accuracy.

V. Conclusions

A combined method of the finite and boundary elements is formulated for the solution of arbitrarily shaped discontinuities in an open dielectric slab waveguide. The discontinuity region is divided into two regions. One is a finite region with arbitrary inhomogeneities, and the other is a semi-infinite and homogeneous region. The FEM and the BEM are applied to the former and the latter region, respectively. For uniform waveguide regions connected to discontinuities, analytical solutions in which both the guided and the radiated modes are taken into account are used.

To show the validity and usefulness of this formulation, computed results are given for a step, a gap, and a triangular rib. For a step, the convergence behavior of the solution is investigated in detail. Convergent values for the reflected and transmitted powers are obtained with sufficient accuracy. The cause of the power conservation error is almost due to the error for the radiated power. When the total normalized power $P_t=1-\epsilon$, we can modify the radiated power P_r as $P_r+\epsilon$.

This approach can be easily extended to discontinuities in an asymmetric slab waveguide.

Appendix

For simplicity the subscript i $(i=1,2)$ is abbreviated.

A. Guided Modes

$$f_m(y)=\frac{1}{\sqrt{D_m}}h_m(y) \tag{A1}$$

$$g_m(y)=\frac{1}{\sqrt{D_m}}\frac{h_m(y)}{p(y)} \tag{A2}$$

$$D_m=\int_0^\infty \frac{(h_m(y))^2}{p(y)}\,dy \tag{A3}$$

$$p(y)=\begin{cases} p_1 & (0\leqslant y\leqslant d) \\ p_2 & (d\leqslant y<\infty) \end{cases} \tag{A4}$$

$$h_m(y)=\begin{cases} \cos\kappa_m y & (0\leqslant y\leqslant d) \\ \cos\kappa_m d\exp\{-\gamma_m(y-d)\} & (d\leqslant y<\infty) \end{cases} \tag{A5}$$

where p_j $(j=1,2)$ is 1 for TE modes and n_j^2 for TM modes.

The dispersion relation for β_m is given as

$$\tan\kappa_m d=p_1\gamma_m/p_2\kappa_m \tag{A6}$$

where

$$\kappa_m=\sqrt{n_1^2k_0^2-\beta_m^2} \tag{A7}$$

$$\gamma_m=\sqrt{\beta_m^2-n_2^2k_0^2}\,. \tag{A8}$$

B. Radiated Modes

$$f(\rho, y) = \frac{1}{\sqrt{D(\rho)}} h(\rho, y) \tag{A9}$$

$$g(\rho, y) = \frac{1}{\sqrt{D(\rho)}} \frac{h(\rho, y)}{p(y)} \tag{A10}$$

$$D(\rho)\delta(\rho - \rho') = \int_0^\infty \frac{h(\rho, y)h(\rho', y)}{p(y)}\, dy \tag{A11}$$

$$h(\rho, y) = \begin{cases} \cos\kappa(\rho)\, y & (0 \leqslant y \leqslant d) \\ \cos\kappa(\rho)\, d \cos\rho(y - d) & \\ \quad - \dfrac{p_2\kappa(\rho)}{p_1\rho} \sin\kappa(\rho)\, d \sin\rho(y - d) & \\ & (d \leqslant y < \infty) \end{cases} \tag{A12}$$

$$\beta(\rho) = \begin{cases} \sqrt{n_2^2 k_0^2 - \rho^2} & (0 \leqslant \rho \leqslant n_2 k_0) \\ -j\sqrt{\rho^2 - n_2^2 k_0^2} & (n_2 k_0 \leqslant \rho < \infty) \end{cases} \tag{A13}$$

$$\kappa(\rho) = \sqrt{(n_1^2 - n_2^2)k_0^2 + \rho^2} \tag{A14}$$

where $\delta(\rho - \rho')$ is the Dirac δ function.

C. Orthonormal Conditions

$$\int_0^\infty f_m(y)\, g_{m'}(y)\, dy = \delta_{mm'} \tag{A15}$$

$$\int_0^\infty f_m(y)\, g(\rho, y)\, dy = 0 \tag{A16}$$

$$\int_0^\infty f(\rho, y)\, g(\rho', y)\, dy = \delta(\rho - \rho'). \tag{A17}$$

References

[1] D. Marcuse, "Radiation losses of tapered dielectric slab waveguides," *Bell Syst. Tech. J.*, vol. 49, pp. 273–290, Feb. 1970.

[2] P. J. B. Clarricoats and A. B. Sharpe, "Modal matching applied to a discontinuity in a planar surface waveguide," *Electron. Lett.*, vol. 8, pp. 28–29, Jan. 1972.

[3] G. A. Hockham and A. B. Sharpe, "Dielectric-waveguide discontinuities," *Electron. Lett.*, vol. 8, pp. 230–231, May 1972.

[4] S. F. Mahmoud and J. C. Beal, "Scattering of surface waves at a dielectric discontinuity on a planar waveguide." *IEEE Trans. Microwave Theory Tech.*, vol. MTT-23, pp. 193–198, Feb. 1975.

[5] G. H. Brooke and M. M. Z. Kharadly, "Step discontinuities on dielectric waveguides," *Electron. Lett.*, vol. 12, pp. 473–475, Sept. 1976.

[6] T. E. Rozzi, "Rigorous analysis of the step discontinuity in a planar dielectric waveguide," *IEEE Trans. Microwave Theory Tech.*, vol. MTT-26, pp. 738–746, Oct. 1978.

[7] T. E. Rozzi and G. H. in't Veld, "Field and network analysis of interacting step discontinuities in planar dielectric waveguides," *IEEE Trans. Microwave Theory Tech.*, vol. MTT-27, pp. 303–309, Apr. 1979.

[8] K. Morishita, S. Inagaki, and N. Kumagai, "Analysis of discontinuities in dielectric waveguides by means of the least squares boundary residual method," *IEEE Trans. Microwave Theory Tech.*, vol. MTT-27, pp. 310–315, Apr. 1979.

[9] PH. Gelin, M. Petenzi, and J. Citerne, "New rigorous analysis of the step discontinuity in a slab dielectric waveguide," *Electron. Lett.*, vol. 15, pp. 355–356, June 1979.

[10] S. Sawa, K. Ono, H. Odaka, and M. Sakuma, "Analysis of tapered optical slab waveguides with hypothetical boundaries," (in Japanese) *Trans. Inst. Electron. Commun. Eng. Japan*, vol. J63-C, pp. 104–111, Feb. 1980.

[11] T. Yoneyama and S. Nishida, "Approximate solution for step discontinuity in dielectric slab waveguide," *Electron. Lett.*, vol. 17, pp. 151–153, Feb. 1981.

[12] T. Hosono, T. Hinata, and A. Inoue, "Numerical analysis of the discontinuities in slab dielectric waveguides," *Radio Sci.*, vol. 17, pp. 75–83, Jan.–Feb. 1982.

[13] G. H. Brooke and M. M. Z. Kharadly, "Scattering by abrupt discontinuities on planar dielectric waveguides," *IEEE Trans. Microwave Theory Tech.*, vol. MTT-30, pp. 760–770, May 1982.

[14] Y. Hayashi, T. Kitazawa, and M. Suzuki, "Analysis of discontinuities in dielectric slab waveguide by means of the induced dipole method," (in Japanese) *Trans. Inst. Electron. Commun. Eng. Japan*, vol. J65-B, pp. 829–835, July 1982.

[15] T. Takenaka and O. Fukumitsu, "Accurate analysis of the abrupt discontinuty in a dielectric waveguide," *Electron. Lett.*, vol. 19, pp. 806–808, Sept. 1983.

[16] K. Uchida and K. Aoki, "Scattering of surface waves on transverse discontinuities in symmetrical three-layer dielectric waveguides," *IEEE Trans. Microwave Theory Tech.*, vol. MTT-32, pp. 11–19, Jan. 1984.

[17] P. G. Cottis and N. K. Uzunoglu, "Analysis of longitudinal discontinuities in dielectric slab waveguides," *J. Opt. Soc. Amer. A*, vol. 1, pp. 206–215, Feb. 1984.

[18] V. Ramaswamy and P. G. Suchoski, Jr., "Power loss at a step discontinuity in an asymmetrical dielectric slab waveguide," *J. Opt. Soc. Amer. A*, vol. 1, pp. 754–759, July 1984.

[19] S. Ray and R. Mittra, "Numerical analysis of open waveguide discontinuities," *Radio Sci.*, vol. 19, pp. 1289–1293, Sept.–Oct. 1984.

[20] H. M. de Ruiter, "Radiation from the junction of two open waveguide sections," *Radio Sci.*, vol. 19, pp. 1295–1300, Sept.–Oct. 1984.

[21] M. Tsuji and H. Shigesawa, "A study on analytical methods of discontinuity problem in open dielectric waveguides," in *1985 National Convention Record* (Institute of Electronics and Communication Engineers of Japan, Yokohama, 1985), no. 782.

[22] H. Shigesawa and M. Tsuji, "Mode propagation through a step discontinuity in dielectric planar waveguide," *IEEE Trans. Microwave Theory Tech.*, vol. MTT-34, pp. 205–212, Feb. 1986.

[23] L. R. Gomaa, "Beam propagation method applied to a step discontinuity in dielectric planar waveguides," *IEEE Trans. Microwave Theory Tech.*, vol. MTT-36, pp. 791–792, Apr. 1988.

[24] N. Morita, "An integral equation method for electromagnetic scattering of guided modes by boundary deformations of dielectric slab waveguides," *Radio Sci.*, vol. 18, pp. 39–47, Jan.–Feb. 1983.

[25] T. Nobuyoshi, N. Morita, and N. Kumagai, "Analysis of the optical waveguide junctions by means of integral equation method," (in Japanese) *Trans. Inst. Electron. Commun. Eng. Japan*, vol. J66-C, pp. 828–834, Nov. 1983.

[26] E. Nishimura, N. Morita, and N. Kumagai, "Theoretical investigation of a gap coupling of two dielectric slab waveguides with arbitrarily shaped ends," (in Japanese) *Trans. Inst. Electron. Commun. Eng. Japan*, vol. J67-C, pp. 714–721, Oct. 1984.

[27] E. Nishimura, N. Morita, and N. Kumagai, "An integral equation approach to electromagnetic scattering from arbitrarily shaped junctions between multilayered dielectric planar waveguides," *J. Lightwave Technol.*, vol. LT-3, pp. 887–894, Aug. 1985

[28] M. Koshiba and M. Suzuki, "Boundary-element analysis of dielectric slab waveguide discontinuities," *Appl. Opt.*, vol. 25, pp. 828–829, Mar. 1986.

[29] M. Suzuki and M. Koshiba, "Finite element analysis of discontinuity problems in a planar dielectric waveguide," *Radio Sci.*, vol. 17, pp. 85–91, Jan.-Feb. 1982.

[30] K. Hirayama, M. Koshiba, and M. Suzuki, "Finite-element analysis of discontinuities in a dielectric slab waveguide," (in Japanese) *Trans. Inst. Electron. Commun. Eng. Japan*, vol. J68-B, pp. 1250–1258, Nov. 1985.

[31] K. Hirayama, M. Koshiba, and M. Suzuki, "Finite-element analysis of dielectric slab waveguide with finite periodic corrugation," (in

Japanese) *Trans. Inst. Electron. Commun. Eng. Japan*, vol. J69-C, pp. 724–730, June 1986.
[32] M. Koshiba and K. Hirayama, "Application of finite-element method to arbitrarily shaped discontinuities in a dielectric slab waveguide," *Proc. Inst. Elec. Eng.*, pt. H, vol. 135, pp. 8–12, Feb. 1988.
[33] O. C. Zienkiewicz, *The Finite Element Method*, 3rd ed. London: McGraw-Hill, 1977.
[34] M. Koshiba and M. Suzuki, "Application of the boundary-element method to waveguide discontinuities," *IEEE Trans. Microwave Theory Tech.*, vol. MTT-34, pp. 301–307, Feb. 1986.
[35] H. Takahasi and M. Mori, "Double exponential formulas for numerical integration," *Publications of the Research Institute for Mathematical Science*, Kyoto University, vol. 9, pp. 721–741, 1974.

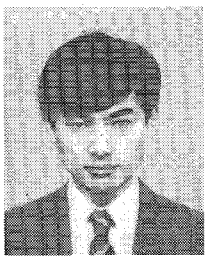

Koichi Hirayama was born in Shiranuka, Hokkaido, Japan, on September 8, 1961. He received the B.S. and M.S. degrees in electronic engineering from Hokkaido University, Sapporo, Japan, in 1984 and 1986, respectively. He is presently studying toward the D.S. degree in electronic engineering at Hokkaido University.

Mr. Hirayama is a member of the Institute of Electronics, Information and Communication Engineers (IEICE).

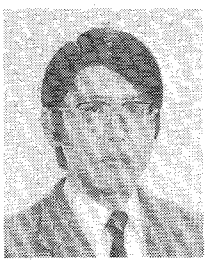

Masanori Koshiba (SM'84) was born in Sapporo, Japan, on November 23, 1948. He received the B.S., M.S., and Ph.D. degrees in electronic engineering from Hokkaido University, Sapporo, Japan, in 1971, 1973, and 1976, respectively.

In 1976, he joined the Department of Electronic Engineering, Kitami Institute of Technology, Kitami, Japan. From 1979 to 1987, he was an Associate Professor of Electronic Engineering at Hokkaido University, and in 1987 he became a Professor. He has been engaged in research on lightwave technology, surface acoustic waves, magnetostatic waves, microwave field theory, and applications of finite-element and boundary-element methods to field problems.

Dr. Koshiba is a member of the Institute of Electronics, Information and Communication Engineers (IEICE), the Institute of Television Engineers of Japan, the Institute of Electrical Engineers of Japan, the Japan Society for Simulation Technology, and the Japan Society for Computational Methods in Engineering. In 1987, he was awarded the 1986 Paper Award by the IEICE.